Single-enzyme biomineralization of cadmium sulfide nanocrystals with controlled optical properties

Robert Dunleavy[a], Li Lu[b], Christopher J. Kiely[a,b], Steven McIntosh[a,1,2], and Bryan W. Berger[a,c,1,2]

[a]Department of Chemical and Biomolecular Engineering, Lehigh University, Bethlehem, PA 18015; [b]Department of Materials Science and Engineering, Lehigh University, Bethlehem, PA 18015; and [c]Program in Bioengineering, Lehigh University, Bethlehem, PA 18015

Edited by Galen D. Stucky, University of California, Santa Barbara, CA, and approved April 4, 2016 (received for review December 2, 2015)

Nature has evolved several unique biomineralization strategies to direct the synthesis and growth of inorganic materials. These natural systems are complex, involving the interaction of multiple biomolecules to catalyze biomineralization and template growth. Herein we describe the first report to our knowledge of a single enzyme capable of both catalyzing mineralization in otherwise unreactive solution and of templating nanocrystal growth. A recombinant putative cystathionine γ-lyase (smCSE) mineralizes CdS from an aqueous cadmium acetate solution via reactive H_2S generation from L-cysteine and controls nanocrystal growth within the quantum confined size range. The role of enzymatic nanocrys-tal templating is demonstrated by substituting reactive Na_2S as the sulfur source. Whereas bulk CdS is formed in the absence of the enzyme or other capping agents, nanocrystal formation is ob-served when smCSE is present to control the growth. This dual-function, single-enzyme, aerobic, and aqueous route to functional material synthesis demonstrates the powerful potential of engi-neered functional material biomineralization.

cadmium sulfide | quantum dot | biomineralization | enzyme | nanoparticle

Biological systems have evolved a diverse array of mechanisms to synthesize inorganic materials from aqueous solutions under ambient conditions. This inherent control over material properties has created interest in using these biological routes to synthesize materials (1–3) such as biosilica from sponges and diatoms (4–8), biogenic $CaCO_3$ from mollusks (9–12), and magnetic particles from magnetotactic bacteria (13–15). Designing a biomineraliza-tion strategy requires control of both the material composition and structure; in nature, this control is typically achieved through the assembly of a multiprotein complex, including both structure-directing proteins and proteins responsible for mineralization of a specific composition. In the current work, we demonstrate the reduction of this complexity to its simplest form: a single enzyme capable of both catalyzing CdS mineralization and controlling particle size within the quantum confined size range to form functional biomineralized CdS quantum dots.

Two of the most studied biomineralization proteins are perlucin and silicatein. Perlucin (16) has been shown to mineralize crystalline forms of $CaCO_3$, a common structural material that constitutes the shell of many marine organisms, in the form of organic–inorganic composites. The role of the nacre protein perlucin in crystallite templating has been elucidated through experiments demonstrating crystallite formation in the presence of purified perlucin, and perlucin selectively being removed from solution during crystallite formation in the presence of a mixture of water-soluble, nacre-associated pro-teins (17). Native silicatein harvested from sea sponge or engineered forms produced recombinantly are active for biomineralization of silica and titania into structures that are amorphous or crystalline (7, 18, 19). In particular, biomineralization confined within an inverse micelle using an engineered silicatein has been demonstrated to form crystalline nanomaterials (20).

With regard to semiconducting metal sulfides, the majority of prior reports have used biological components to template structure during synthesis from reactive sulfur precursors, typically Na_2S (21–23). For example, peptides displayed on the surface of bacteriophage have been used to produce intricately ordered CdS and ZnS nanowires (24), whereas engineered viral particles (25, 26) along with recombinant, self-assembled cage-like proteins (27) have served as nucleation cavities for CdS nanocrystals. Spoerke and Voigt (21) engineered a library of CdS-capping peptides capable of templating CdS nanocrystal growth from cadmium acetate and Na_2S, with the resulting optical properties dependent on the chemical structure of the capping peptide. Singh et al. (28) engi-neered bifunctional peptides with CdSe- and ZnS-binding domains for the synthesis of CdSe/ZnS core shell nanoparticles by the re-action of $CdCl_2$ with NaHSe followed by the addition of $ZnCl_2$ and Na_2S. Harvested natural phytochelatins (22) or engineered cell-based methods to produce phytochelatins (29) have also been de-veloped for the synthesis of CdS nanoparticles. Another intriguing approach is the use of a self-assembled ribbon-like template to control synthesis of CdS nanohelices (30). To the best of our knowledge, the only example of enzymatic production of a reactive sulfur species is that of a sulfite reductase (31) reducing Na_2SO_3 to generate larger, 5–20 nm, CdS nanoparticles by using additional templating peptides. That is, the enzyme does not template the crystal growth.

We previously identified a putative cystathionine γ-lyase (smCSE) associated with the extracellular synthesis of CdS quantum dot nanocrystals by Stenotrophomonas maltophilia strain SMCD1 (32). Cystathionine γ-lyases (CSEs) are a class of enzymes that catalyze the production of H_2S, NH_3 and pyruvate from L-cysteine, and the overexpression of which has been shown to precipitate cadmium sulfide (33). In this study, we demonstrate the putative smCSE from S. maltophilia SMCD1 is capable of reactive H_2S generation,

Significance

Biomineralization is a promising, yet complex, route toward the scalable and green biomanufacturing of functional nanomaterials, involving multiple biomolecules acting in unison to control mineralization and crystal structure. Unraveling the interdependent complexity of biomineralization is a barrier to completely realize this approach. We distill this complexity to a single enzyme that both catalyzes the formation of the reactive precursors required for mineralization and templates nanocrystal growth in solution. This is the first report of a single enzyme capable of providing all of the required functionality for active biomineralization from otherwise unreactive solution. This work provides insight into the mechanism of metal sulfide biomineralization and is an example of the elegance in green functional material synthesis achievable through engineered biomineralization.

Author contributions: R.D., L.L., C.J.K., S.M., and B.W.B. designed research; R.D., L.L., C.J.K., S.M., and B.W.B. performed research; R.D., L.L., C.J.K., S.M., and B.W.B. contributed new reagents/analytic tools; R.D., L.L., C.J.K., S.M., and B.W.B. analyzed data; and R.D., L.L., C.J.K., S.M., and B.W.B. wrote the paper.

The authors declare no conflict of interest.

This article is a PNAS Direct Submission.

[1]S.M. and B.W.B. contributed equally to this work.

[2]To whom correspondence may be addressed. Email: bwb209@lehigh.edu or stm310@lehigh.edu.

consistent with its function as a cystathionine γ-lyase. In addition, the purified smCSE enzyme, by itself, is capable of aqueous phase synthesis of CdS nanocrystals directly from cadmium acetate and L-cysteine. The resulting CdS nanocrystals are within the quantum confined size range and display optoelectronic properties analogous to those previously described for cell-based or chemically synthesized CdS nanocrystals (21–23, 32, 34–37). When the substrate L-cysteine is replaced by the chemical precursor Na_2S, smCSE is capable of directing CdS nanocrystal formation in solution. Removal of smCSE results in bulk CdS formation, indicating a role for smCSE not only in H_2S gener-ation, but also in templating CdS nanocrystals. Therefore smCSE is capable of synthesizing metal sulfide nanocrystals directly from aqueous solution, opening up a wide range of strategies for engineering the biomineralization of functional materials.

A Putative smCSE Associated with Biosynthetic Quantum Dots Is Capable of H_2S Generation

Previous studies have shown that overexpressed CSEs are ca-pable of precipitating cadmium sulfide in cell culture (33, 38–42) and suggested that H_2S generation from CSE was the pri-mary driver for CdS precipitation. To determine whether the putative CSE identified from S. maltophilia (smCSE) was ca-pable of H_2S generation from L-cysteine, smCSE was heterol-ogously overexpressed and purified from Escherichia coli and the intrinsic kinetics of L-cysteine turnover to H_2S measured (described in SI Appendix, SI Materials and Methods). Expres-sion and purification using immobilized metal affinity chroma-tography yielded a single protein of 42 kDa (SI Appendix, Fig. S1), consistent with the expected size of smCSE (NCBI reference no. WP_012509966.1). The purified smCSE also shows a strong ab-sorbance peak at 430 nm (SI Appendix, Fig. S1), which is indicative of a covalently bound pyridoxal 5′ phosphate (PLP) cofactor; PLP is an obligate cofactor required for CSE catalysis (43). The Michaelis–Menten rate parameters for L-cysteine turnover mea-sured for smCSE using L-cysteine as a substrate are consistent with reported values for other well-characterized CSEs (44, 45) (SI Appendix, Fig. S1).

The Quantum Dot-Associated smCSE Regulates CdS Nanocrystal Growth and Size

Having established the ability of smCSE to generate reactive sulfur species, it was hypothesized that the addition of a cad-mium salt to the solution would yield CdS. To test this hy-pothesis, L-cysteine (4 mM) and cadmium acetate (0.5 mM) were added to an aqueous solution of smCSE (0.1 mg/mL in Tris buffer, pH 7.5), and the solution was monitored by using UV-visible and fluorescence spectroscopy as a function of time at ambient temperature and pressure (Fig. 1). After 90 min, a distinct absorbance peak was observed with an absorbance maximum at 333 nm (Fig. 1A). A corresponding fluorescence emission peak at 464 nm was also observed (Fig. 1B). The maxima of both absorbance and fluorescence progressively shift to longer wavelengths over the course of 195 min (Fig. 1 A and B) with visible photoluminescence observed in solution for each time point measured when illuminated under UV light (Fig. 1C). It should be noted that the presence of smCSE, cadmium acetate, and L-cysteine were all required; omission of any one of these components produced solutions that dis-played no absorbance or fluorescence peaks and no observable photoluminescence when illuminated under UV light (SI Ap-pendix, Fig. S2). Placing the reactant mixture on ice essen-tially arrests smCSE activity, allowing a specific population of particles with a given set of photoluminescent properties to be collected.

Enzymatically Synthesized CdS Quantum Dots Are Monodisperse and Crystalline

Crystallites were harvested from solution after 180 min of growth (absorbance maximum at 350 nm) and analyzed via scanning transmission electron microscopy (STEM). Fig. 2A shows the existence of discrete, but irregularly shaped and overlapping, nanocrystals between 2–4 nm in diameter. Elemental analysis

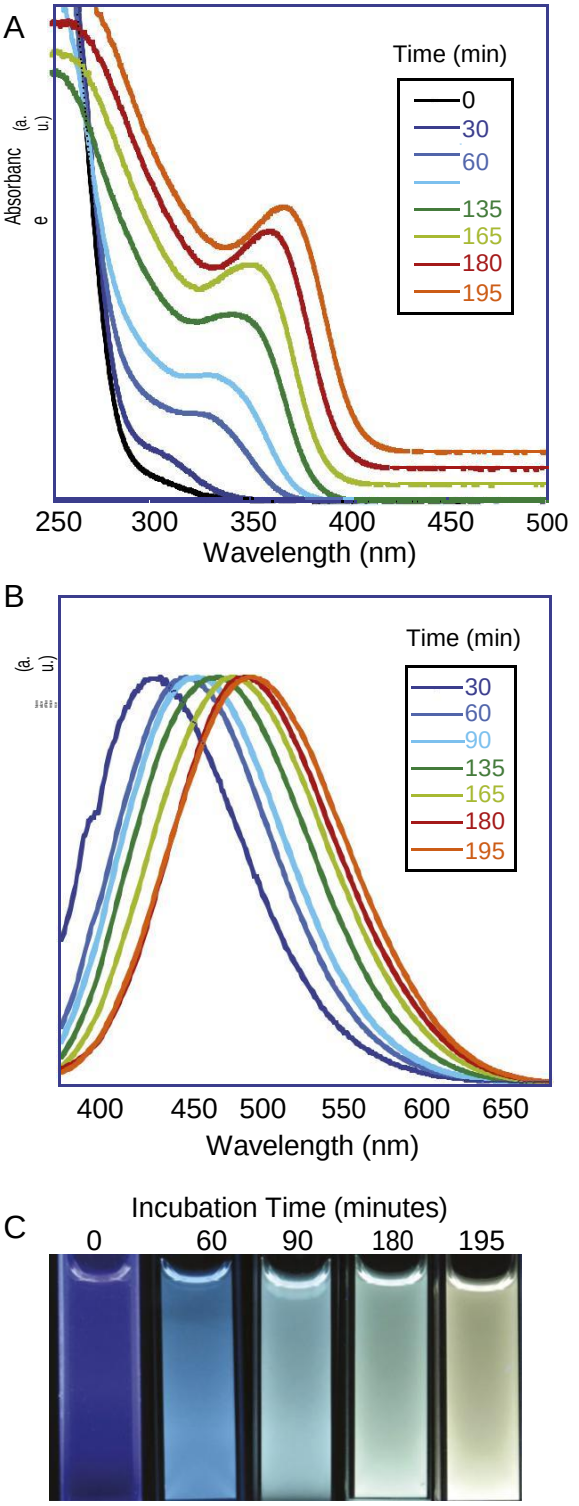

Fig. 1. Optical properties of CdS versus synthesis time. (A) Absorbance spectra of smCSE (0.1 mg/mL) incubated with 4 mM L-cysteine and 0.5 mM cadmium acetate for various time intervals. (B) Corresponding fluorescence spectra at selected time intervals using an excitation wavelength of 350 nm. (C) Photo-graphs of photoluminescence under UV light at various time intervals. The red shift of the absorbance and fluorescence maxima indicates an increase in the mean size of the CdS nanocrystals with incubation time.

from this region using X-ray energy-dispersive spectroscopy (XEDS) (Fig. 2B) reveals strong Cd and S signals. The presence of strong Cu and C peaks are artifacts arising from the copper mesh TEM grid coated with a carbon film. High-resolution high-angle annular dark field (HAADF) imaging of individual and isolated particles confirms the size of the nanocrystals and the presence of both wurtzite (Fig. 2 C and D) and zinc-blende structured (Fig. 2 E and F) nanocrystals. The lattice parameters and interplanar angles of these crystals are consistent with those for CdS (SI Appendix, Tables S1 and S2). These lattice parameters and both crystalline phases have been observed for chemically and biologically synthesized CdS nanocrystals (21, 36). Powder X-ray diffraction measurements (SI Appendix, Fig. S3) on material harvested after 12 h growth is also consistent with the presence of both structures of CdS.

The irregular shape of the biomineralized nanocrystals prevents a precise comparison with reported literature correlations (46) for the optical properties as a function of particle diameter. However, for all reported growth times, the absorbance maximum (Fig. 1A) remains well below the absorbance maximum corresponding to the band gap of bulk CdS (2.5 eV, 495 nm) (47, 48) and the observed biomineralized CdS nanocrystals size is well within the quantum confined size range for CdS (47). The observed red shift in optical properties with growth time (Fig. 1 A and B) is indicative of CdS nanocrystal growth as a function of time within this quantum-confined size range. For reference, our previous work (32) demonstrated that absorption peak maxima of 324, 334, and 344 nm correspond to biomineralized nanocrystallite sizes of 2.75 ± 0.68, 3.04 ± 0.75, and 3.36 ± 0.95 nm, respectively. Additionally, smCSE-produced CdS nanocrystals show similar quantum yield (1.8%) compared with synthesized CdS nanocrystals from S. maltophilia (2%) (32).

CdS Quantum Dot Growth Depends on both H_2S Production and Available Capping Agents

Although L-cysteine is a substrate for smCSE to generate H_2S, it can also act as an aqueous phase capping agent for CdS (34). To confirm the dual role of L-cysteine as the sulfur source and capping agent, CdS biomineralization was studied as a function of L-cysteine concentration. At a concentration of 4 mM L-cysteine, found to be the practical lower limit for nanocrystal synthesis at 0.1 mg/mL smCSE and 0.5 mM cadmium acetate, the observed optical absorbance maximum increases with time, reaching 370 nm after 4 h of growth (Fig. 3A); longer growth times beyond 4 h led to formation of bulk CdS with an absorbance maximum consistent with bulk CdS (SI Appendix, Fig. S4). Increasing L-cysteine concen-tration to 10 and 20 mM red shifts the absorbance maximum and corresponding photoluminescence during growth (Fig. 3 A and B).

This red shift is indicative of an increase in CdS growth rate with increasing L-cysteine concentration for nanocrystals within the quantum confined size range and is particularly noticeable for the 20 mM L-cysteine data. Interestingly, all of the growth curves reach similar maxima after 4 h: 370, 375, and 380 nm at 4, 10, and 20 mM L-cysteine, respectively. At longer growth times the solutions lose optical clarity, indicating a maximum in the solubility of the presumably L-cysteine–capped nanocrystals; images of solutions illuminated by using UV light at each L-cysteine concentration and growth time are given in Fig. 3B to demonstrate optical clarity at each solution condition.

To further demonstrate that thiol-mediated capping is impor-tant for stabilizing the nanocrystals, glutathione was introduced into the enzymatic synthesis mixture. Glutathione is a capping agent derived from L-cysteine and L-glutamine that has been shown previously to stabilize water-soluble CdS nanocrystals (22, 49). However, unlike L-cysteine, glutathione is not a substrate for CSEs (50) and, therefore, acts solely as a capping agent. No nanocrystal formation was observed in the absence of L-cysteine which clearly demonstrates that L-cysteine is the sulfur source for the nano-crystal growth through the enzymatic generation of H_2S.

In the presence of 4 mM L-cysteine, 1 and 4 mM glutathione addition yielded growth curves and absorbance maxima at 4 h (375 and 385 nm for 1 and 4 mM glutathione, respectively), similar to those with elevated L-cysteine concentration, although the solutions maintain optical clarity after 5 h of growth (Fig. 3 C and D). This retention of optical clarity is indicative of increased stabilization of the aqueous nanocrystal solution with the gluta-thione capping agent versus L-cysteine capping agent. Although the 4 mM glutathione growth curve shows some indication of a decreased growth rate, this phenomenon is clearly observed upon increasing the glutathione concentration to 10 mM. Compared with lower glutathione concentrations, the 10 mM glutathione growth curve shows a blue shift in absorbance maximum at all growth times and yields an optically clear so-lution with absorbance maximum at 400 nm after 24 h of growth (Fig. 3 C and D).

To further demonstrate the role of glutathione as a capping agent, the absorbance maximum and L-cysteine concentration were measured as a function of time (SI Appendix, Fig. S5) in the presence and absence of glutathione. Whereas L-cysteine deg-radation is not influenced by the presence of glutathione, the absorbance maximum occurs at lower wavelength, indicating a smaller average particle size, for the glutathione containing sample. This reduction in average size is consistent with the capping role envisioned for glutathione because an increased capping agent concentration will lead to smaller average particle size. Where the

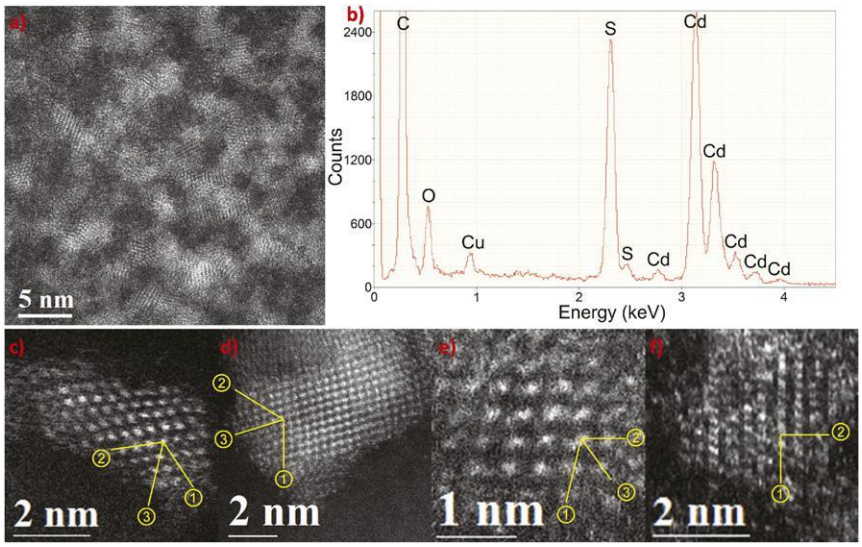

Fig. 2. HAADF-STEM characterization of smCSE-synthesized nanocrystals. Representative image show-ing numerous dispersed but overlapping nanocrystals (A); XEDS spectrum confirming the coexistence of Cd and S in the nanocrystals (B); example images from wurtzite CdS nanocrystals viewed along [101] and [211] projections, respectively (C and D); example images from zinc-blende CdS nanocrystals viewed along [110] and [211] projections, respectively (E and F).

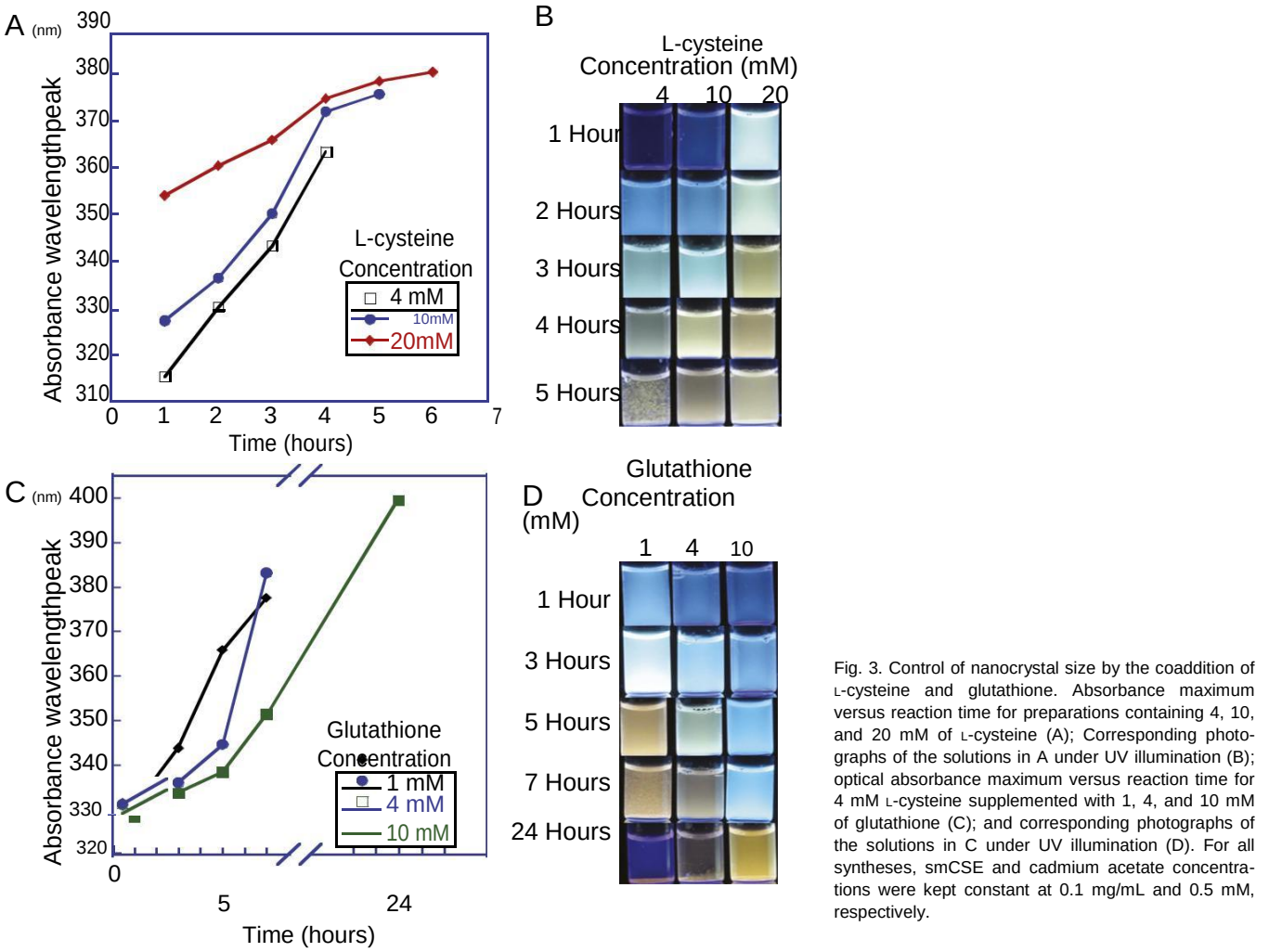

Fig. 3. Control of nanocrystal size by the coaddition of L-cysteine and glutathione. Absorbance maximum versus reaction time for preparations containing 4, 10, and 20 mM of L-cysteine (A); Corresponding photographs of the solutions in A under UV illumination (B); optical absorbance maximum versus reaction time for 4 mM L-cysteine supplemented with 1, 4, and 10 mM of glutathione (C); and corresponding photographs of the solutions in C under UV illumination (D). For all syntheses, smCSE and cadmium acetate concentrations were kept constant at 0.1 mg/mL and 0.5 mM, respectively.

L-cysteine concentration-dependent stabilization and growth of CdS nanocrystals is due to its role as both a capping agent and substrate for smCSE, addition of a thiolated capping agent gluta-thione that is not a substrate for smCSE stabilizes the nanocrystal solution and shifts the crystal growth curve to a lower average size at a given time.

smCSE Regulates CdS Nanocrystal Growth and Size Independent of H_2S Generation

To ascertain the role of smCSE in directing the structure and size of the CdS nanocrystals, L-cysteine was replaced with Na_2S to act as the sulfur source. Na_2S is not a substrate for smCSE, such that H_2S will not be produced by smCSE under these conditions, but Na_2S is a sulfur source in the aqueous chemical synthesis of CdS nanocrystals in the presence of thiolated ligand capping agents (35). Addition of Na_2S (4 mM) to an aqueous solution of cadmium acetate (0.5 mM) at room temperature leads to nearly instantaneous formation of large aggregates of bulk CdS, with no distinct absorbance maximum (Fig. 4A) or photoluminescence (Fig. 4B). This immediate formation of bulk material is due to the lack of a capping agent to control nano-crystal growth. However, when smCSE (0.1 mg/mL) is added to the solution, a distinct absorbance maximum rapidly emerges at 360 nm (Fig. 4A), indicating the formation of CdS nanocrystals. The formation of CdS nanocrystals in the absence of the sub-strate L-cysteine clearly indicates the role of smCSE in tem-plating and controlling the growth of CdS nanocrystals.

Absorbance and photoluminescence characteristics indicative of nanocrystal formation were also observed if known capping agents L-cysteine or glutathione were present (Fig. 4 A and B). The absorption maxima for the glutathione and L-cysteine capping ligands are sharper, which likely reflects their higher affinity for the particle surface and their smaller size, both of which lead to higher coverage on the particle surface during growth (21, 51). Thus, in all three cases, smCSE, L-cysteine, and glutathione act as structure directing agents to form CdS nanocrystals, rather than bulk CdS, from Na_2S and cadmium acetate. Therefore smCSE has the intrinsic ability to regulate CdS nanocrystal growth independently from, and in addition to, its role in reactive H_2S generation (Fig. 4C).

Discussion

This work clearly demonstrates the ability of a single enzyme (smCSE) to produce both crystalline CdS (Fig. 2) and regulate growth to form nanocrystals within the quantum confined size range (Fig. 1). Previous studies involving enzymatic or peptide-based biomineralization of metal sulfide nanoparticles have demonstrated either CdS formation from enzymatically generated H_2S without intrinsic size control (31, 33), or have demonstrated nanocrystal size control by adding specific peptides or proteins and use reactive Na_2S as a sulfur source (21–23). As an example, Wang et al. overexpressed Treponema denticola CSE in E. coli (33) and demonstrated that aqueous cadmium ions were removed under aerobic growth conditions. In this instance, the flux of H_2S from the cell surface led to the nucleation and growth of CdS precipi-tates over the course of 48 h without apparent size control. An alternative example used engineered overexpression of cysteine-rich phytochelatin peptides in E. coli (29), which are known to sequester metal ions in solution, to produce 3–4 nm CdS nanocrystals in E. coli cells in the presence of the reactant Na_2S. In contrast, smCSE acts

both as the sulfur generating source to mineralize CdS (Fig. 1) and as a structure directing agent to control nanocrystal growth (Fig. 4). Thus, smCSE efficiently combines mineralization and templating into a single enzyme (smCSE; Fig. 4C) that are engineered separately in other biomineralization strategies.

The combination of H_2S generation and controlled growth afforded by smCSE is remarkable compared with other enzymatic and peptide approaches to nanocrystal synthesis. In the presence of excess capping agents (L-cysteine or glutathione) under conditions where smCSE can generate H_2S, we find that the CdS nanocrystals can span a range of quantum confined sizes and resulting optical properties (Fig. 3). Reducing the amount or quality of capping agent limits the stability of the resulting colloidal solution (Fig. 3). It is noted that the addition of capping agents L-cysteine or glutathione appear to improve the nanocrystal quality as well through providing capping agents with smaller size and higher affinity for the particle surface (21, 51). Independent of its role in H_2S generation, smCSE is also capable of templating CdS nanocrystals from solution when using chemical precursors such as Na_2S (Fig. 4), to exhibit intrinsic structure directing and capping activity similar to naturally occurring phy-tochelatins (22, 23, 29) or nanocrystal-binding peptides (21, 24, 28).

In a previous study using the protein pepsin as a templating agent (52), the rate of reactive sulfur generation and subsequent nanocrystal synthesis was at least an order of magnitude slower than that of smCSE (days versus hours). This rate is dictated by the slow, spontaneous hydrolysis of thioacetamide to generate reactive sulfur, in contrast to the smCSE-catalyzed H_2S gener-ation demonstrated in this work.

Given the intrinsic heavy metal resistance of S. maltophilia (41), our results would suggest that smCSE secretion may be one of several independent mechanisms of heavy metal resistance used by microorganisms to both sequester metal ions and convert them into insoluble precipitates outside of the cell. The strategy demonstrated herein distills the potential complexity of biomineralization down to its simplest form: a single enzyme. The ongoing challenge is to develop strategies that enable a wider range of materials synthesis.

In summary, an engineered smCSE is capable of controlled CdS nanocrystal synthesis directly from aqueous solution by us-ing L-cysteine and cadmium acetate as reactants. Furthermore, the ability of smCSE to mineralize CdS and template nanocrystal formation provides a single enzyme route for engineered nanocrystal biomineralization.

Materials and Methods

Expression, Purification, and Kinetics of Recombinant CSE. An E. coli codon-optimized form of the putative S. maltophilia CSE (Smal_0489; Genscript) was subcloned into pET28a (+) and transformed in BL21 cells with expression and purification as described (53). Detection of H_2S product formation using the substrate L-cysteine to determine Michaelis–Menten rate parameters was performed as described (54).

Cadmium Sulfide Nanocrystal Biosynthesis. smCSE (0.1 mg/mL) was incubated with 0.5 mM cadmium acetate and 4 mM L-cysteine in 100 mM Tris buffer (pH 7.5). CdS nanocrystal formation was directly observed in solution as a function of time by illumination using a UV lamp. Absorbance spectra for CdS nanocrystals were taken at regular time intervals on a Shimadzu UV-Vis 3300 spectrometer, and fluorescence emission spectra were measured on a PTI QuantaMaster fluorimeter with a 350-nm excitation wavelength by using a 5-nm excitation slit width. To demonstrate the ability of CSE to control CdS nanocrystal growth and size in-dependent of H_2S generation, Na_2S was added instead of L-cysteine to a final concentration of 4 mM in a solution containing 0.5 mM cadmium acetate and 0.1 mg/mL CSE. Absorbance and fluorescence spectra as well as direct observation of solutions under UV light were used to characterize the optical properties of the CdS nanoparticles in solution.

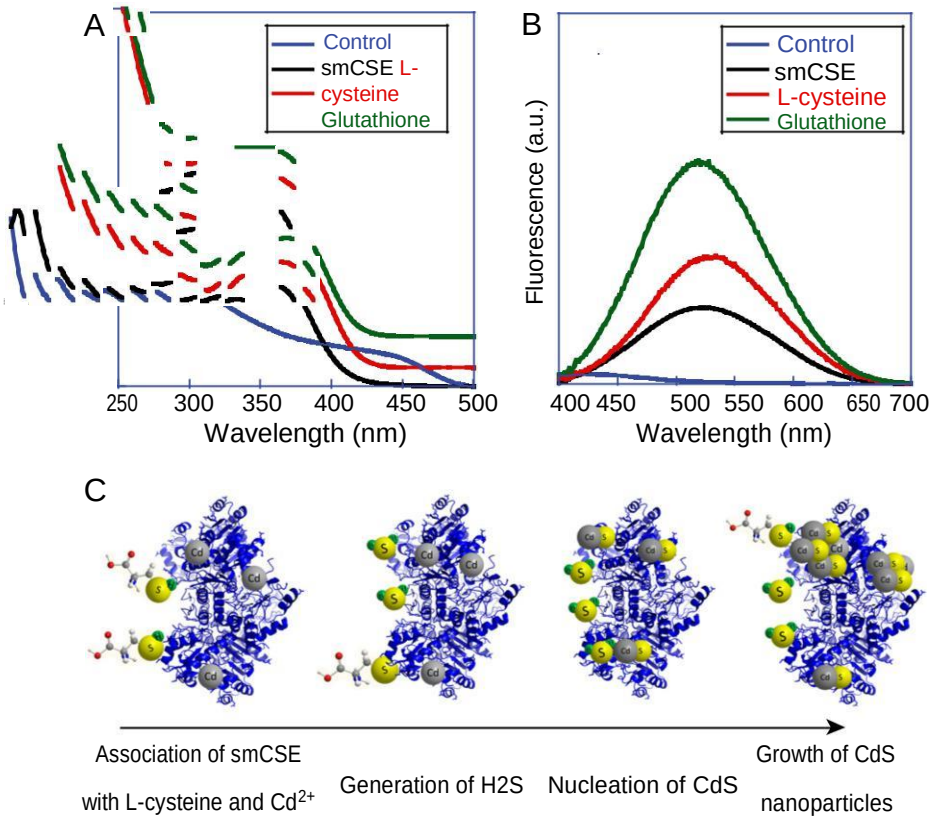

Fig. 4. smCSE forms nanocrystals in the absence of L-cysteine or glutathione. (A) UV-visible absorbance spectra obtained upon the addition of 4 mM Na_2S to a preparation containing 0.5 mM cadmium acetate in the presence of smCSE, 4 mM L-cysteine, or 4 mM glutathione. A solution of Na_2S added to 0.5 mM cadmium acetate is shown as a control. (B) Corresponding fluorescence (excitation at 360 nm) of solutions in A. (C) Schematic of proposed CdS quantum dot synthesis by smCSE. smCSE associates with cadmium acetate and L-cysteine present in solution, smCSE degrades L-cysteine to produce H_2S, H_2S produced by smCSE nucleates CdS nanoparticles, and CdS nanoparticles continue to grow upon the continuous generation of H_2S.

X-Ray Diffraction. Incubation of CSE with cadmium acetate and L-cysteine for 16– 24 h led to the formation of solutions of CdS particles displaying optical charac-teristics indicative of bulk as opposed to nanoscale material (SI Appendix, Fig. S4). This bulk CdS was collected by centrifugation and washed twice with absolute ethanol and dried under ambient conditions. Powder XRD spectra were taken of the resultant dried material on a Rigaku Miniflex II Diffractometer by using Cu K_α (1.542 Å) radiation. Spectra were compared with standard XRD patterns for wur-zite type CdS (PDF card no. 00-006-0314) and zinc blende type CdS (PDF card no. 00-010-0454) from the International Centre for Diffraction Data (ICDD) database.

Transmission Electron Microscopy. Biosynthetic CdS nanocrystals were grown for 3 h, corresponding to an absorbance maximum at 350 nm, and subsequently dialyzed at 4 °C against a reservoir containing 0.5 mM L-cysteine for 24 h. The dialyzed CdS nanocrystals solutions were placed dropwise onto Ar plasma-treated carbon-coated copper TEM grids and the liquid evaporated under vacuum. High resolution (HR)-TEM and HAADF-STEM images were taken on a 200-kV aberration corrected JEOL ARM 200CF analytical electron microscope equipped with a Centurio XEDS system.

ACKNOWLEDGMENTS. This material presented is the result of research work supported by the National Science Foundation under Emerging Frontiers in Research and Innovation-Photosynthetic Bioreactor (EFRI-PSBR) Program Grant 1332349 and the Lehigh University Collaborative Research Opportu-nity program (R.D.)

1. Mann S (2001) Biomineralization: Principles and Concepts in Bioinorganic Materials Chemistry (Oxford Univ Press, New York).
2. Dickerson MB, Sandhage KH, Naik RR (2008) Protein- and peptide-directed syntheses of inorganic materials. Chem Rev 108(11):4935–4978.
3. Nudelman F, Sommerdijk NA (2012) Biomineralization as an inspiration for materials chemistry. Angew Chem Int Ed Engl 51(27):6582–6596.
4. Kröger N, Deutzmann R, Bergsdorf C, Sumper M (2000) Species-specific polyamines from diatoms control silica morphology. Proc Natl Acad Sci USA 97(26):14133–14138.
5. Kröger N, Deutzmann R, Sumper M (1999) Polycationic peptides from diatom biosilica that direct silica nanosphere formation. Science 286(5442):1129–1132.
6. Sumper M, Brunner E (2006) Learning from diatoms: Nature's tools for the production of nanostructured silica. Adv Funct Mater 16(1):17–26.
7. Shimizu K, Cha J, Stucky GD, Morse DE (1998) Silicatein alpha: Cathepsin L-like protein in sponge biosilica. Proc Natl Acad Sci USA 95(11):6234–6238.
8. Müller WEG, Krasko A, Le Pennec G, Schröder HC (2003) Biochemistry and cell biology of silica formation in sponges. Microsc Res Tech 62(4):368–377.
9. Falini G, Albeck S, Weiner S, Addadi L (1996) Control of Aragonite or calcite poly-morphism by mollusk shell macromolecules. Science 271(5245):67–69.
10. Addadi L, Raz S, Weiner S (2003) Taking advantage of disorder: Amorphous calcium carbonate and its roles in biomineralization. Adv Mater 15(12):959–970.
11. Zaremba CM, et al. (1996) Critical transitions in the biofabrication of abalone shells and flat pearls. Chem Mater 8(3):679–690.
12. Belcher AM, et al. (1996) Control of crystal phase switching and orientation by soluble mollusc-shell proteins. Nature 381:56–58.
13. Lang C, Schüler D, Faivre D (2007) Synthesis of magnetite nanoparticles for bio- and nanotechnology: Genetic engineering and biomimetics of bacterial magnetosomes. Macromol Biosci 7(2):144–151.
14. Scheffel A, et al. (2006) An acidic protein aligns magnetosomes along a filamentous structure in magnetotactic bacteria. Nature 440(7080):110–114.
15. Faivre D, Schüler D (2008) Magnetotactic bacteria and magnetosomes. Chem Rev 108(11):4875–4898.
16. Wang N, Lee Y-H, Lee J (2008) Recombinant perlucin nucleates the growth of calcium carbonate crystals: Molecular cloning and characterization of perlucin from disk ab-alone, Haliotis discus discus. Comp Biochem Physiol B Biochem Mol Biol 149(2): 354–361.
17. Blank S, et al. (2003) The nacre protein perlucin nucleates growth of calcium car-bonate crystals. J Microsc 212(Pt 3):280–291.
18. Tahir MN, et al. (2004) Monitoring the formation of biosilica catalysed by histidine-tagged silicatein. Chem Commun (Camb) (24):2848–2849.
19. Tahir MN, et al. (2005) Formation of layered titania and zirconia catalysed by surface-bound silicatein. Chem Commun (Camb) (44):5533–5535.
20. Bawazer LA, et al. (2012) Evolutionary selection of enzymatically synthesized semi-conductors from biomimetic mineralization vesicles. Proc Natl Acad Sci USA 109(26): E1705–E1714.
21. Spoerke ED, Voigt JA (2007) Influence of engineered peptides on the formation and properties of cadmium sulfide nanocrystals. Adv Funct Mater 17(13):2031–2037.
22. Bae W, Mehra RK (1998) Properties of glutathione- and phytochelatin-capped CdS bionanocrystallites. J Inorg Biochem 69(1-2):33–43.
23. Liu F, et al. (2010) Enzyme mediated synthesis of phytochelatin-capped CdS nano-crystals. Appl Phys Lett 97:123703.
24. Mao C, et al. (2003) Viral assembly of oriented quantum dot nanowires. Proc Natl Acad Sci USA 100(12):6946–6951.
25. Flynn CE, et al. (2003) Synthesis and organization of nanoscale II-VI semiconductor materials using evolved peptide specificity and viral capsid assembly. J Mater Chem 13(10):2414–2421.
26. Zhou Z, Bedwell GJ, Li R, Prevelige PE, Jr, Gupta A (2014) Formation mechanism of chalcogenide nanocrystals confined inside genetically engineered virus-like particles. Sci Rep 4:3832.
27. Iwahori K, et al. (2007) Cadmium sulfide nanoparticle synthesis in Dps protein from Listeria innocua. Chem Mater 19(13):3105–3111.
28. Singh S, Bozhilov K, Mulchandani A, Myung N, Chen W (2010) Biologically pro-grammed synthesis of core-shell CdSe/ZnS nanocrystals. Chem Commun (Camb) 46(9): 1473–1475.
29. Kang SH, Bozhilov KN, Myung NV, Mulchandani A, Chen W (2008) Microbial synthesis of CdS nanocrystals in genetically engineered E. coli. Angew Chem Int Ed Engl 47(28): 5186–5189.
30. Sone ED, Zubarev ER, Stupp SI (2005) Supramolecular templating of single and double nanohelices of cadmium sulfide. Small 1(7):694–697.
31. Ansary AA, et al. (2007) CdS quantum dots: Enzyme mediated in vitro synthesis, characterization and conjugation with plant lectins. J Biomed Nanotechnol 3(4): 406–413.
32. Yang Z, et al. (2015) Biomanufacturing of CdS quantum dots. Green Chem 17(7): 3775–3782.
33. Wang CL, Lum AM, Ozuna SC, Clark DS, Keasling JD (2001) Aerobic sulfide production and cadmium precipitation by Escherichia coli expressing the Treponema denticola cysteine desulfhydrase gene. Appl Microbiol Biotechnol 56(3-4):425–430.
34. Piven NG, Khalavka YB, Shcherbak LP (2008) Effect of SH-containing ligands on the growth of CdS nanoparticles. Inorg Mater 44(10):1047–1051.
35. Winter JO, Gomez N, Gatzert S, Schmidt CE, Korgel BA (2005) Variation of cadmium sulfide nanoparticle size and photoluminescence intensity with altered aqueous synthesis conditions. Colloids Surf A Physicochem Eng Asp 254(1-3):147–157.
36. Li H, Shih WY, Shih WH (2007) Synthesis and characterization of aqueous carboxyl-capped CdS quantum dots for bioapplications. Ind Eng Chem Res 46(7):2013–2019.
37. Sweeney RY, et al. (2004) Bacterial biosynthesis of cadmium sulfide nanocrystals. Chem Biol 11(11):1553–1559.
38. Edwards CD, Beatty JC, Loiselle JBR, Vlassov KA, Lefebvre DD (2013) Aerobic trans-formation of cadmium through metal sulfide biosynthesis in photosynthetic micro-organisms. BMC Microbiol 13:161.
39. Bai HJ, Zhang ZM, Guo Y, Yang GE (2009) Biosynthesis of cadmium sulfide nano-particles by photosynthetic bacteria Rhodopseudomonas palustris. Colloids Surf B Biointerfaces 70(1):142–146.
40. Gallardo C, et al. (2014) Low-temperature biosynthesis of fluorescent semiconductor nanoparticles (CdS) by oxidative stress resistant Antarctic bacteria. J Biotechnol 187: 108–115.
41. Pages D, et al. (2008) Heavy metal tolerance in Stenotrophomonas maltophilia. PLoS One 3(2):e1539.
42. Cunningham DP, Lundie LL, Jr (1993) Precipitation of cadmium by Clostridium ther-moaceticum. Appl Environ Microbiol 59(1):7–14.
43. Matsuo Y, Greenberg DM; Prosthetic Group (1958) A crystalline enzyme that cleaves homoserine and cystathionine. II. Prosthetic group. J Biol Chem 230(2):561–571.
44. Sun Q, et al. (2009) Structural basis for the inhibition mechanism of human cys-tathionine gamma-lyase, an enzyme responsible for the production of H(2)S. J Biol Chem 284(5):3076–3085.
45. Yano T, Fukamachi H, Yamamoto M, Igarashi T (2009) Characterization of L-cysteine desulfhydrase from Prevotella intermedia. Oral Microbiol Immunol 24(6):485–492.
46. Yu WW, Qu L, Guo W, Peng X (2003) Experimental determination of the extinction coefficient of CdTe, CdSe, and CdS nanocrystals. Chem Mater 15(14):2854–2860.
47. Alivisatos A (1996) Semiconductor clusters, nanocrystals, and quantum dots. Science 271(5251):933–937.
48. Einevoll GT (1992) Confinement of excitons in quantum dots. Phys Rev B Condens Matter 45(7):3410–3417.
49. Thangadurai P, Balaji S, Manoharan PT (2008) Surface modification of CdS quantum dots using thiols-structural and photophysical studies. Nanotechnology 19(43): 435708.
50. Collins JM, Monty KJ (1973) The cysteine desulfhydrase of Salmonella typhimurium. Kinetic and catalytic properties. J Biol Chem 248(17):5943–5949.
51. Jiang C, Xu S, Yang D, Zhang F, Wang W (2007) Synthesis of glutathione-capped CdS quantum dots and preliminary studies on protein detection and cell fluorescence image. Luminescence 22(5):430–437.
52. Yang L, Shen Q, Zhou J, Jiang K (2005) Biomimetic synthesis of CdS nanocrystals in aqueous solution of pepsin. Mater Lett 59:2889–2892.
53. Petty KJ (2001) Metal-chelate affinity chromatography. Curr Protoc Protein Sci 4(9.4): 9.4.1–9.4.16.
54. Chiku T, et al. (2009) H2S biogenesis by human cystathionine gamma-lyase leads to the novel sulfur metabolites lanthionine and homolanthionine and is responsive to the grade of hyperhomocysteinemia. J Biol Chem 284(17):11601–11612.